AIMS Mathematics, 11(8): 23588–23605.
DOI: 10.3934/math.2026950
Received: 15 June 2026
Revised: 16 July 2026
Accepted: 27 July 2026
Published: 03 August 2026

https://www.aimspress.com/journal/Math

*Research article*

# Effects of diffusion and advection on endemic steady states in a partially degenerate West Nile virus model

**Jie Xing**[1,2] **and Lin Wang**[3,*]

[1] School of Mathematics and Computing Science, Guilin University of Electronic Technology, Guilin 541002, Guangxi, China
[2] Center for Applied Mathematics of Guangxi (GUET), Guilin 541002, Guangxi, China
[3] School of Science, Jimei University, Xiamen 361021, Fujian, China

* **Correspondence:** Email: lwang133@jmu.edu.cn.

**Abstract:** This paper studies endemic steady states of a partially degenerate West Nile virus model in a bounded one-dimensional heterogeneous habitat. The infected bird population is subject to diffusion and directional advection, whereas the infected mosquito density is determined at steady state by a local host-vector transmission balance. This leads to an elliptic-algebraic steady-state problem rather than a fully diffusive system. We first reduce the system to a scalar elliptic boundary value problem and prove the existence and uniqueness of a positive endemic steady state by the method of upper and lower solutions. We then examine how the diffusion rate and the advection rate affect the endemic spatial profile. In the advection-dominated regime, including large advection and vanishing diffusion with fixed positive advection, the infected bird density forms a downstream boundary layer, and the limiting boundary value is determined by a scalar equation. In the large-diffusion regime, the infected bird density converges to a positive spatially homogeneous state and the infected mosquito density is obtained from the local transmission relation. Numerical simulations are presented to illustrate these diffusion-advection effects on the spatial distribution of infection.

**Keywords:** West Nile virus model; partially degenerate system; endemic steady states; advection effect; boundary layer
**Mathematics Subject Classification:** 35K57, 35B40, 92D25

## 1. Introduction

West Nile virus (WNV) is a mosquito-borne arbovirus of the family *Flaviviridae*. In nature, WNV is mainly maintained through a transmission cycle involving birds and mosquitoes, especially *Culex* mosquitoes, while humans and horses are generally considered incidental hosts [11, 14, 17]. Since

its first isolation in Uganda in 1937 [14], WNV has been reported in a broad range of ecological settings, and its spatial spread has motivated extensive epidemiological and mathematical studies. From a public-health perspective, the absence of a widely available human vaccine or specific antiviral treatment makes prevention largely dependent on surveillance, mosquito control, and reduction of mosquito exposure. These facts do not by themselves determine disease outcomes, but they make it meaningful to understand how host-vector interactions, spatial heterogeneity, and movement processes affect the persistence and spatial distribution of infection.

Mathematical models have played an important role in clarifying the transmission mechanisms of WNV. Early compartmental models and their extensions described the interaction between infected birds and mosquitoes, identified threshold quantities, (e.g., the basic reproduction number), and investigated the stability of disease-free and endemic equilibria [1, 7, 8, 15, 17]. Such models provide useful qualitative criteria for persistence and extinction. However, WNV transmission is inherently spatial: birds and mosquitoes move in heterogeneous environments, and ecological factors, such as habitat structure, local vector abundance, mortality, and transmission rates, may vary across space. This motivates the use of reaction-diffusion and advection models, which allow one to examine how random dispersal, directional movement, and spatially varying coefficients influence disease spread and long-term infection patterns [5, 9, 10, 18].

Advection is particularly relevant in spatial models for WNV because bird movement and wind-assisted transport may introduce directional bias into the spread of infection. Maidana and Yang [13] studied traveling waves in a WNV model and showed that avian dispersal and wind-driven advection can have a substantial influence on spreading speed. Lin and Zhu [10] introduced a free-boundary reaction-diffusion model for WNV and derived spreading-vanishing criteria in terms of appropriate risk indices. Ge et al. [5] further considered a heterogeneous advective environment and analyzed the effects of avian diffusion and advection when mosquito movement is neglected. These studies indicate that directional transport and spatial heterogeneity can alter the spatial range and persistence of infection. At the same time, most of the above works focus on time-dependent spreading dynamics, threshold behavior, or free-boundary propagation, while the detailed spatial profiles of positive steady states, especially under extreme diffusion or advection regimes, remain less well understood.

Recently, Xing et al. [18] investigated a bounded-domain WNV model with spatial heterogeneity and advection. The model takes the form

$$\begin{cases} H_t = DH_{xx} - \alpha H_x + \dfrac{\beta_h(x)V(N_h^* - H)}{N_h^*} - (\mu_h(x) + r)H, & x \in (0, L), t > 0, \\ V_t = \dfrac{\beta_v(x)H(N_v^* - V)}{N_h^*} - \mu_v(x)(1 - q)V, & x \in (0, L), t > 0, \\ DH_x(0, t) - \alpha H(0, t) = DH_x(L, t) - \alpha H(L, t) = 0, & t > 0. \end{cases} \tag{1.1}$$

Here $H(x, t)$ and $V(x, t)$ denote the densities of infected birds and infected mosquitoes, respectively. The parameter $D > 0$ represents the diffusion rate of infected birds, and $\alpha \geq 0$ measures the strength of directional advection. The constants $N_h^*$ and $N_v^*$ denote the total bird and mosquito populations, respectively. $\beta_h(x), \beta_v(x), \mu_h(x)$ and $\mu_v(x)$ are positive Hölder continuous functions. Specifically, the functions $\beta_h(x)$ and $\beta_v(x)$ describe the transmission rates from infected mosquitoes to susceptible birds and from infected birds to susceptible mosquitoes, while $\mu_h(x)$ and $\mu_v(x)$ denote the corresponding mortality rates. The parameter $r$ is the recovery rate of infected birds, and $0 < q \ll 1$ represents

the vertical transmission probability in mosquitoes [2]. The boundary condition in (1.1) is a no-flux condition for the advective bird population, describing an isolated one-dimensional habitat. Xing et al. [18] derived the basic reproduction number of the aforementioned time-dependent reaction-diffusion-advection model and established threshold dynamics, as well as uniform persistence results. Their work further provides a complete long-time dynamical classification in the $D$-$\alpha$ parameter plane by partitioning the recovery parameter $r$. Nevertheless, their analysis exclusively focuses on transient evolutionary behaviors of the time-dependent system, leaving the existence, uniqueness, and extreme-regime asymptotic shapes of positive endemic steady states unexplored.

To fill this research gap, the present paper turns full attention to the following steady-state counterpart of system (1.1):

$$\begin{cases} DH_{xx} - \alpha H_x + \dfrac{\beta_h(x)V(N_h^* - H)}{N_h^*} - (\mu_h(x) + r)H = 0, & x \in (0, L), \\ \dfrac{\beta_v(x)H(N_v^* - V)}{N_h^*} - \mu_v(x)(1-q)V = 0, & x \in (0, L), \\ DH_x(0) - \alpha H(0) = DH_x(L) - \alpha H(L) = 0. \end{cases} \tag{1.2}$$

This system is partially degenerate: diffusion and advection act directly on the infected bird component, whereas the mosquito component is governed by a local algebraic balance at steady state. This structure is biologically consistent with a modeling assumption in which infected bird movement is the dominant spatial process, while mosquito infection responds locally to bird infection and environmental coefficients. For example, the mean dispersal distance for Aedes aegypti was ranged from 28 to 199 m, proposed by Harrington et al. [6]. Mathematically, however, this partial degeneracy prevents one from directly applying standard compactness arguments for fully diffusive cooperative systems. Therefore, even when persistence of the corresponding time-dependent problem is known, the existence, uniqueness, and limiting profiles of positive steady states require a separate analysis.

The purpose of this paper is to determine how diffusion and advection affect endemic steady states of (1.2). In the present WNV model, a positive steady state represents a persistent spatial infection profile involving infected birds and infected mosquitoes. By solving the mosquito equation explicitly in terms of the infected bird density, we reduce the steady-state system to a scalar elliptic boundary value problem. Under a natural positivity condition, we prove the existence and uniqueness of a positive endemic steady state by the method of upper and lower solutions. We then characterize the effects of the movement parameters on the endemic profile. When advection dominates diffusion, either through large advection or through vanishing diffusion with fixed positive advection, the infected bird density is asymptotically concentrated near the downstream boundary and is described by an exponential boundary-layer profile. Moreover, the limiting boundary value is determined by a scalar equation. In contrast, when diffusion becomes large, the infected bird density converges to a positive spatially homogeneous state. The infected mosquito density is then recovered from the local host-vector transmission relation. These results complement the threshold dynamics obtained in [18]: Threshold results determine whether infection persists, whereas the present analysis describes how the persistent infection is spatially distributed and how this distribution changes with diffusion and advection.

The biological implications of these mathematical results should be interpreted cautiously. The model is not intended to provide quantitative predictions for a particular field site without parameter

calibration. Rather, it offers a qualitative framework for understanding how directional movement and diffusion may shape the spatial distribution of infected hosts and vectors in a heterogeneous bounded habitat. In particular, the boundary-layer result suggests that strong directional transport may produce localized accumulation of infection, whereas large diffusion tends to reduce spatial variation. Such conclusions may be useful when interpreting spatial risk patterns or designing more detailed models that incorporate site-specific ecological data.

The remainder of this paper is organized as follows. Section 2 establishes the existence and uniqueness of positive solutions to (1.2). Section 3 derives the limiting endemic profiles under diffusion and advection, including the downstream boundary-layer limit and the large-diffusion homogenization limit. Section 4 presents numerical simulations and discusses their consistency with the analytical results. Section 5 concludes the paper with a brief discussion of the main findings and possible extensions.

## 2. Existence and uniqueness

We first consider the following eigenvalue problem with advection:

$$\begin{cases} D\phi_{xx} + \alpha\phi_x + m(x)\phi = \lambda\phi, & x \in (0, L), \\ \phi_x(0) = \phi_x(L) = 0. \end{cases} \tag{2.1}$$

It follows from the Krein-Rutman theorem that system (2.1) admits a principal eigenvalue, denoted by $\lambda_1(D, \alpha)$, which corresponds to a positive eigenfunction $\phi_1$ normalized by $\max_{x\in[0,L]} \phi_1(x) = 1$. Furthermore, by the variational characterization of the principal eigenvalue, we have

$$\lambda_1(D, \alpha) = \sup_{\phi\in H^1((0,L))\setminus\{0\}} \frac{-D\int_0^L e^{\frac{\alpha}{D}x}\phi_x^2 \mathrm{d}x + \int_0^L e^{\frac{\alpha}{D}x} m(x)\phi^2 \mathrm{d}x}{\int_0^L e^{\frac{\alpha}{D}x}\phi^2 \mathrm{d}x}. \tag{2.2}$$

By the above variational characterization (2.2) and [16, Proposition 3.2], we obtain the following results.

**Lemma 2.1.** *(See [16, Proposition 3.2]) The following results hold for $\lambda_1(D, \alpha)$:*

(i) *If $\int_0^L e^{\frac{\alpha}{D}x} m(x)\mathrm{d}x > 0$, then $\lambda_1(D, \alpha) > 0$ for all $D > 0, \alpha \geq 0$.*
(ii) *If $m(x) < 0$ on $[0, L]$, then $\lambda_1(D, \alpha) < 0$ for all $D > 0, \alpha \geq 0$.*

Then, we are ready to show the existence and uniqueness of the steady-state solutions of system (1.2). From the second equation of (1.2), we obtain

$$V = \frac{\beta_v(x)N_v^* H}{\mu_v(x)(1-q)N_h^* + \beta_v(x)H}.$$

Substituting it into the first equation of (1.2), we obtain the following single-species system:

$$\begin{cases} DH_{xx} - \alpha H_x + H\left(\dfrac{\beta_h(x)\beta_v(x)N_v^*(N_h^* - H)}{N_h^*(\mu_v(x)(1-q)N_h^* + \beta_v(x)H)} - (\mu_h(x) + r)\right) = 0, \ x \in (0, L), \\ DH_x(0) - \alpha H(0) = DH_x(L) - \alpha H(L) = 0. \end{cases} \tag{2.3}$$

Let $\mathcal{H} = e^{-\frac{\alpha}{D}x}H$. Then, it follows from (2.3) that $\mathcal{H}$ satisfies

$$\begin{cases} D\mathcal{H}_{xx} + \alpha\mathcal{H}_x + \mathcal{H}\Big(\frac{\beta_h(x)\beta_v(x)N_v^*(N_h^* - e^{\frac{\alpha}{D}x}\mathcal{H})}{N_h^*\big(\mu_v(x)(1-q)N_h^* + \beta_v(x)e^{\frac{\alpha}{D}x}\mathcal{H}\big)} - (\mu_h(x) + r)\Big) = 0, \quad x \in (0, L), \\ \mathcal{H}_x(0) = \mathcal{H}_x(L) = 0. \end{cases} \tag{2.4}$$

Linearizing system (2.4) at $\mathcal{H} = 0$, we obtain the following eigenvalue problem:

$$\begin{cases} D\varphi_{xx} + \alpha\varphi_x + \Big(\frac{\beta_h(x)\beta_v(x)N_v^*}{\mu_v(x)(1-q)N_h^*} - (\mu_h(x) + r)\Big)\varphi = \eta\varphi, \quad x \in (0, L), \\ \varphi_x(0) = \varphi_x(L) = 0. \end{cases} \tag{2.5}$$

Similarly, we denote the principal eigenvalue and eigenfunction of problem (2.5) by $\eta_1(D, \alpha)$ and $\varphi_1$, respectively. Next, we prove the existence of positive solutions to system (2.3). Let

$$\Theta(x) = \frac{\beta_h(x)\beta_v(x)N_v^*}{N_h^*\mu_v(x)(1-q)}, \quad \theta(x) = \Theta(x) - \mu_h(x),$$

and define $\theta^* := \min_{x\in[0,L]} \theta(x)$.

**Lemma 2.2.** *Let $\theta^* > 0$ and $0 < r < \theta^*$. Then, for any $D > 0$ and $\alpha \geq 0$, system* (2.3) *admits a unique positive solution $H^*(x)$. Moreover, $H^*(x)$ satisfies*

$$0 < H^*(x) \leq e^{\frac{2\alpha L}{D}}N_h^*.$$

*Proof.* To establish the existence and uniqueness of positive solutions to (2.3), it is sufficient to prove the unique positive solvability of the auxiliary equation (2.4).

If $0 < r < \theta^*$, then $\theta(x) - r > 0$ holds for all $x \in [0, L]$. Combining this with Lemma 2.1, we obtain $\eta_1(D, \alpha) > 0$ for all $D > 0$ and $\alpha \geq 0$. Accordingly, for sufficiently small $\epsilon > 0$, the function $\epsilon\varphi_1$ serves as a lower solution of (2.4).

Define the nonlinear function

$$g(\mathcal{H}) := \frac{N_v^*\beta_h(x)\beta_v(x)(N_h^* - e^{\frac{\alpha}{D}x}\mathcal{H})}{N_h^*\Big(\mu_v(x)(1-q)N_h^* + \beta_v(x)e^{\frac{\alpha}{D}x}\mathcal{H}\Big)} - (\mu_h(x) + r).$$

One can readily verify that the constant $C^* := e^{\frac{\alpha L}{D}}N_h^*$ satisfies $g(\mathcal{H}) < 0$ for all $\mathcal{H} \geq C^*$. This indicates that $C^*$ constitutes an upper solution of (2.4). By virtue of the classical upper-lower solution method (see [3, Proposition 3.2]), the auxiliary system (2.4) admits at least one positive solution $\mathcal{H}^*(x)$.

Furthermore, direct computation yields

$$g'(\mathcal{H}) = \frac{-N_v^*\beta_h(x)\beta_v(x)e^{\frac{\alpha}{D}x}(\mu_v(x)(1-q) + \beta_v(x))}{\Big(\mu_v(x)(1-q)N_h^* + \beta_v(x)e^{\frac{\alpha}{D}x}\mathcal{H}\Big)^2} < 0.$$

The strict monotonicity of $g(\mathcal{H})$, together with [3, Proposition 3.3], guarantees that $\mathcal{H}^*(x)$ is the unique positive solution of (2.4) and satisfies $0 < \mathcal{H}^*(x) \leq C^*$. Hence, $0 < \mathcal{H}^*(x) \leq e^{\frac{\alpha L}{D}}N_h^*$. Finally, the positive solution of the original system (2.3) is recovered via the variable transformation $\mathcal{H} = e^{-\frac{\alpha}{D}x}H$, which completes the proof. □

With the results in Lemma 2.2, we immediately have the following result for system (1.2).

**Theorem 2.3.** *Let $\theta^* > 0$ and $0 < r < \theta^*$. Then, for any $D > 0$ and $\alpha \geq 0$, system* (1.2) *has a unique positive solution $(H^*(x), V^*(x))$, where*

$$V^*(x) = \frac{N_v^*\beta_v(x)H^*(x)}{\mu_v(x)(1-q)N_h^* + \beta_v(x)H^*(x)},$$

*and $H^*(x)$ is the unique positive solution of* (2.3).

**Remark 2.4.** *As established in [18, Theorem 3.8], system* (1.1) *is $\kappa$-contracting, where $\kappa$ denotes the Kuratowski measure of noncompactness [4], and is uniformly persistent for $0 < r < \theta^*$. Nevertheless, [12, Theorem 4.7] cannot be applied to prove the existence of positive steady-state solutions of* (1.1)*, as it requires the solution semigroup to be $\kappa$-condensing. The lack of compactness induced by the single-diffusion structure renders classical approaches for steady-state existence and uniqueness invalid. To address this issue, we establish the existence and uniqueness of positive steady-state solutions for system* (1.2) *via the upper-lower solution method.*

## 3. Limiting endemic profiles under diffusion and advection

In this section, we investigate how the diffusion rate, $D$, and the advection rate, $\alpha$, affect the endemic steady state obtained in Theorem 2.3. In particular, we derive the boundary-layer limit in the advection-dominated regime and the homogenization limit in the large-diffusion regime.

To this end, we first show that $(H^*(x), V^*(x))$ depends continuously differentiably on the diffusion rate, $D$, and the advection rate, $\alpha$.

**Lemma 3.1.** *For any $D > 0$ and $\alpha \geq 0$, the positive solution $(H^*(x), V^*(x))$ of system* (1.2) *is continuously differentiable with respect to $D$ and $\alpha$.*

*Proof.* We first establish continuous differentiability of $(H^*(x), V^*(x))$ with respect to the advection rate $\alpha$. From the algebraic relation

$$V^*(x) = \frac{N_v^*\beta_v(x)H^*(x)}{\mu_v(x)(1-q)N_h^* + \beta_v(x)H^*(x)},$$

it suffices to verify the continuous differentiability of $H^*(x)$ in $\alpha$. For a fixed value of $\alpha$, define the operator $F\colon C_B^2([0,L]) \to C([0,L])$ by

$$F(\alpha, H) = DH_{xx} - \alpha H_x + H\left(\frac{\beta_h(x)\beta_v(x)N_v^*(N_h^* - H)}{N_h^*(\mu_v(x)(1-q)N_h^* + \beta_v(x)H)} - (\mu_h(x) + r)\right),$$

where

$$C_B^2([0,L]) = \{H \in C^2([0,L]) \,\big|\, DH_x(0) - \alpha H(0) = DH_x(L) - \alpha H(L) = 0\}.$$

Equivalently, one may work with the transformed Neumann problem (2.4), whose boundary conditions are independent of $\alpha$. The corresponding nonlinear operator is $C^1$, and Lemma 2.2 yields $F(\alpha, H^*) = 0$. Direct computation gives the Fréchet derivative

$$\frac{\partial F}{\partial H}(\alpha, H^*) = D\frac{d^2}{dx^2} - \alpha\frac{d}{dx} + \left(\frac{N_v^*\beta_h(x)\beta_v(x)(N_h^* - H^*(x))}{N_h^*(\mu_v(x)(1-q)N_h^* + \beta_v(x)H^*(x))} - (\mu_h(x) + r)\right) - f(x),$$

with

$$f(x) = H^*(x)\frac{N_v^*\beta_h(x)\beta_v(x)\big(\mu_v(x)(1-q)+\beta_v(x)\big)}{\big(\mu_v(x)(1-q)N_h^*+\beta_v(x)H^*(x)\big)^2} > 0, \quad x \in [0, L].$$

Recalling (2.4), one has

$$\eta_1\left(D, \alpha, \frac{N_v^*\beta_h(x)\beta_v(x)(N_h^* - H^*(x))}{N_h^*(\mu_v(x)(1-q)N_h^* + \beta_v(x)H^*(x))} - (\mu_h(x)+r)\right) = 0.$$

Combining this identity with the explicit form of $\partial F/\partial H(\alpha, H^*)$, the principal eigenvalue of the Fréchet operator is strictly negative, which guarantees that zero is not an eigenvalue. An application of the implicit function theorem [3, Theorem 3.5] together with compactness reasoning ensures the existence of a $C^1$-mapping $H(\alpha^*)\colon \mathbb{R}^+ \to C_B^2([0, L])$ satisfying $H(\alpha^*)|_{\alpha^*=\alpha} = H^*$ and $F(\alpha^*, H(\alpha^*)) = 0$. By local uniqueness of solutions near $(\alpha, H^*)$, $H(\alpha^*) = H^*$ whenever $\alpha^* = \alpha$. Hence $H^*$ depends continuously differentiably on $\alpha \in [0, +\infty)$.

(ii) Now fix $\alpha$ and vary $D > 0$. A key difference from Case 1: the boundary condition $DH_x - \alpha H = 0$ defines a space $C_B^2(D)$ that changes with $D$, so we cannot directly apply the implicit function theorem on a fixed Banach space. To resolve this, perform the change of variable $w = DH$, which rewrites the boundary condition as

$$w_x(0) - \alpha w(0) = 0, \qquad w_x(L) - \alpha w(L) = 0,$$

independent of $D$. Substitute $H = w/D$ into the operator $F$ to obtain a new operator $\mathcal{F}(D, w)$ defined on a parameter-independent fixed space

$$C_B^2 = \{w \in C^2[0, L] \mid w_x(0) - \alpha w(0) = w_x(L) - \alpha w(L) = 0\}.$$

The transformed equation $\mathcal{F}(D, w) = 0$ is jointly $C^1$ in $(D, w)$. The Fréchet derivative $\partial_w \mathcal{F}$ inherits the same elliptic structure as $\partial_H F$ above, with strictly negative principal eigenvalue. Hence $\partial_w \mathcal{F}$ is invertible. The implicit function theorem now applies to $\mathcal{F} : \mathbb{R}_+ \times C_B^2 \to C[0, L]$, producing a $C^1$ map $w(D)$. Recovering $H = w/D$, we conclude $H^*$ is continuously differentiable with respect to $D > 0$.

□

Next, we present the uniform boundedness of $H^*(x)$ and $V^*(x)$ with respect to $D$ and $\alpha$.

**Lemma 3.2.** (i) *For fixed $D > 0$, $H^*(x)$ and $V^*(x)$ are uniformly bounded with respect to $\alpha \in [0, +\infty)$.*

(ii) *For fixed $\alpha \geq 0$, $H^*(x)$ and $V^*(x)$ are uniformly bounded with respect to $D \in (0, +\infty)$.*

*Proof.* Since $V^*(x) = \frac{N_v^*\beta_v(x)H^*(x)}{\mu_v(x)(1-q)N_h^*+\beta_v(x)H^*(x)}$, it suffices to prove $H^*(x)$ is uniformly bounded for $\alpha \in [0, +\infty)$.

(i) For fixed $D > 0$, Lemma 2.2 guarantees the uniform boundedness of $H^*(x)$ as $\alpha \to 0^+$. We now establish the uniform boundedness of $H^*(x)$ as $\alpha \to +\infty$. For clarity, the proof is divided into two steps.

**Step 1:** The function $H^*(x)$ is strictly increasing on $[0, L]$. Define the transformation $u = e^{-\frac{\alpha}{2D}x}H^*$. Substituting into (2.3) yields

$$\begin{cases} Du_{xx} + u\left(\frac{N_v^*\beta_h(x)\beta_v(x)(N_h^*-H^*(x))}{N_h^*\left(\mu_v(x)(1-q)N_h^*+\beta_v(x)H^*(x)\right)} - (\mu_h(x)+r) - \frac{\alpha^2}{4D}\right) = 0, \quad x \in (0, L), \\ Du_x(0) - \frac{\alpha}{2}u(0) = Du_x(L) - \frac{\alpha}{2}u(L) = 0. \end{cases}$$

Let $\Theta_M := \max_{x\in[0,L]} \Theta(x)$. For all $\alpha \geq 2\sqrt{D\Theta_M}$, the positivity of $H^*(x)$ implies

$$\frac{N_v^*\beta_h(x)\beta_v(x)(N_h^* - H^*(x))}{N_h^*(\mu_v(x)(1-q)N_h^* + \beta_v(x)H^*(x))} - (\mu_h(x)+r) - \frac{\alpha^2}{4D} < \Theta(x) - \frac{\alpha^2}{4D} \leq \Theta_M - \frac{\alpha^2}{4D} \leq 0.$$

Accordingly, $u_{xx} > 0$ holds for all $x \in [0, L]$. Combining this with the boundary condition $u_x(0) = \frac{\alpha}{2D}H^*(0) > 0$, we obtain $u_x(x) > 0$ for all $x \in [0, L]$. Therefore, direct computation gives

$$H_x^*(x) = \left(\frac{\alpha}{2D}u(x) + u_x(x)\right)e^{\frac{\alpha}{2D}x} > 0, \quad x \in [0, L],$$

which verifies the strict monotonicity of $H^*(x)$.

**Step 2:** $H^*(L)$ is uniformly bounded as $\alpha \to +\infty$. Suppose, for contradiction, that $H^*(L) \to +\infty$ as $\alpha \to +\infty$. By extracting a subsequence if necessary, we introduce the scaled variable $y = \frac{\alpha}{D}(L - x)$ and define the rescaled solutions

$$\mathbf{H}(y) := H^*\left(L - \frac{D}{\alpha}y\right), \qquad \tilde{\mathbf{H}}(y) := \frac{\mathbf{H}(y)}{\mathbf{H}(0)}.$$

It follows that $\tilde{\mathbf{H}}(y)$ satisfies

$$\begin{cases} \tilde{\mathbf{H}}_{yy} + \tilde{\mathbf{H}}_y + \frac{D}{\alpha^2}\tilde{\mathbf{H}}(y)\left[\frac{N_v^*\beta_h(L-\frac{D}{\alpha}y)\beta_v(L-\frac{D}{\alpha}y)(N_h^*-\mathbf{H}(y))}{N_h^*\left(\mu_v(L-\frac{D}{\alpha}y)(1-q)N_h^*+\beta_v(L-\frac{D}{\alpha}y)\mathbf{H}(y)\right)} - (\mu_h(L-\frac{D}{\alpha}y)+r)\right] = 0, \ y \in (0, \frac{\alpha L}{D}), \\ \tilde{\mathbf{H}}_y(0) + \tilde{\mathbf{H}}(0) = \tilde{\mathbf{H}}_y(\frac{\alpha L}{D}) + \tilde{\mathbf{H}}(\frac{\alpha L}{D}) = 0, \ \ \tilde{\mathbf{H}}(0) = 1. \end{cases} \tag{3.1}$$

Clearly, $0 < \tilde{\mathbf{H}}(y) \leq 1$ for all $y \in \left[0, \frac{\alpha L}{D}\right]$. Moreover, the following uniform estimate holds:

$$\begin{aligned} &\left|\frac{N_v^*\beta_h\left(L-\frac{D}{\alpha}y\right)\beta_v\left(L-\frac{D}{\alpha}y\right)(N_h^*-\mathbf{H}(y))}{N_h^*(\mu_v\left(L-\frac{D}{\alpha}y\right)(1-q)N_h^*+\beta_v\left(L-\frac{D}{\alpha}y\right)\mathbf{H}(y))} - \left(\mu_h\left(L-\frac{D}{\alpha}y\right)+r\right)\right| \\ &\leq \Theta\left(L-\frac{D}{\alpha}y\right) + \frac{N_v^*\beta_h\left(L-\frac{D}{\alpha}y\right)}{N_h^*} + \mu_v\left(L-\frac{D}{\alpha}y\right) + r. \end{aligned}$$

Integrating the first equation of (3.1) over $(0, y)$ yields the uniform boundedness of $\tilde{\mathbf{H}}_y$ as $\alpha \to +\infty$. Substituting back into (3.1), we further deduce that $\tilde{\mathbf{H}}_{yy}$ is also uniformly bounded for sufficiently large $\alpha$. By passing to a subsequence if necessary, a subsequence of $\{\tilde{\mathbf{H}}\}$ converges locally in $C^1((0,\infty))$ to a limiting function $\tilde{\mathbf{H}}^*$, which satisfies

$$\tilde{\mathbf{H}}_{yy}^* + \tilde{\mathbf{H}}_y^* = 0, \quad y \in (0,\infty), \quad \tilde{\mathbf{H}}_y^*(0) + \tilde{\mathbf{H}}^*(0) = 0, \quad \tilde{\mathbf{H}}^*(0) = 1.$$

Elementary calculation gives the unique solution $\tilde{\mathbf{H}}^* = e^{-y}$.

Integrating the first equation of (3.1) over $\left(0, \frac{\alpha L}{D}\right)$ leads to

$$\int_0^{\frac{\alpha L}{D}} \tilde{\mathbf{H}}(y)\left(\frac{N_v^*\beta_h\left(L-\frac{D}{\alpha}y\right)\beta_v\left(L-\frac{D}{\alpha}y\right)(N_h^*-\tilde{\mathbf{H}}(y)\mathbf{H}(0))}{N_h^*(\mu_v\left(L-\frac{D}{\alpha}y\right)(1-q)N_h^*+\beta_v\left(L-\frac{D}{\alpha}y\right)\tilde{\mathbf{H}}(y)\mathbf{H}(0))} - (\mu_h(L-\frac{D}{\alpha}y)+r)\right)\mathrm{d}y = 0. \tag{3.2}$$

Before passing to the limit $\alpha \to +\infty$, we justify interchanging the limit and integration over the expanding domain $[0, \frac{\alpha L}{D}]$ via dominated convergence.

The normalized solution satisfies $0 < \tilde{\mathbf{H}}(y) \leq 1$, and the algebraic bracket term is uniformly bounded by a negative constant independent of $\alpha, y$. We find a dominating function $Ce^{-y}$ integrable on $[0, \infty)$ bounding the absolute value of the full integrand. The tail contribution over $y > \frac{\alpha L}{D}$ obeys

$$\left| \int_{\frac{\alpha L}{D}}^{\infty} Ce^{-y} dy \right| = Ce^{-\frac{\alpha L}{D}} \to 0 \quad \text{as } \alpha \to \infty.$$

For any fixed finite threshold $M > 0$, for all sufficiently large $\alpha$ we have $M < \frac{\alpha L}{D}$. On the fixed bounded interval $[0, M]$, every spatially varying coefficient converges pointwise and uniformly:

$$\beta_h\left(L - \tfrac{D}{\alpha}y\right) \to \beta_h(L), \quad \beta_v\left(L - \tfrac{D}{\alpha}y\right) \to \beta_v(L), \quad \mu_{h/v}\left(L - \tfrac{D}{\alpha}y\right) \to \mu_{h/v}(L),$$

and $\tilde{\mathbf{H}}(y) \to e^{-y}$ uniformly on $[0, M]$. The standard dominated convergence theorem applies on the fixed compact set $[0, M]$, allowing us to exchange the limit and finite-range integral.

Combining vanishing tail decay and finite-domain dominated convergence, we may safely take $\alpha \to +\infty$ inside the integral to reach

$$\int_0^{\infty} e^{-y} \left( \frac{N_v^* \beta_h(L) \beta_v(L)(N_h^* - e^{-y}\mathbf{H}(0))}{N_h^*(\mu_v(L)(1-q)N_h^* + \beta_v(L)e^{-y}\mathbf{H}(0))} - (\mu_h(L) + r) \right) \mathrm{d}y = 0. \tag{3.3}$$

Since $\mathbf{H}(0) = H^*(L) \to +\infty$ as $\alpha \to +\infty$, we deduce that

$$\frac{N_v^* \beta_h(L - \frac{D}{\alpha}y)\beta_v(L - \frac{D}{\alpha}y)(N_h^* - \tilde{\mathbf{H}}(y)\mathbf{H}(0))}{N_h^*(\mu_v(L - \frac{D}{\alpha}y)(1-q)N_h^* + \beta_v(L - \frac{D}{\alpha}y)\tilde{\mathbf{H}}(y)\mathbf{H}(0))} - (\mu_h(L - \frac{D}{\alpha}y) + r) < 0$$

for large $\alpha$, which contradicts (3.2). Therefore, $H^*(L)$ must be uniformly bounded as $\alpha \to +\infty$. Together with the monotonicity of $H^*(x)$ on $[0, L]$, we conclude that $H^*(x)$ is uniformly bounded as $\alpha \to +\infty$. Hence, for each fixed $D > 0$, there exists a constant $M^* > 0$ independent of sufficiently large $\alpha$ such that $H^*(x) \leq M^*$ for $x \in [0, L]$. (ii) The proof for the large-diffusion regime is obtained from the equation after division by $D$ and the boundary condition $DH_x - \alpha H = 0$. For the small-diffusion advection-dominated regime used below, the same boundary-layer rescaling as in part (i) yields the required bound. The details are analogous to those in part (i), after replacing the large-advection scaling by the corresponding large- or small-diffusion scaling. □

We now characterize the limiting endemic profiles under diffusion and advection. The next theorem describes two distinct effects: strong advection or vanishing diffusion with fixed positive advection leads to a downstream boundary layer, whereas large diffusion produces spatial homogenization of the infected bird density.

**Theorem 3.3.** *Assume that $\theta^* > 0$ and $0 < r < \theta^*$. Let $D > 0$ and $\alpha \geq 0$. Then, the following statements hold:*

(i) *If either* (a) $D > 0$ *and* $\alpha \to +\infty$, *or* (b) $\alpha > 0$ *is fixed and* $D \to 0^+$, *so that* $\alpha \geq 2\sqrt{D\Theta_M}$ *for all sufficiently small D, where* $\Theta_M = \max_{x \in [0,L]} \Theta(x)$, *then* $\|(H^*(x), V^*(x)) - (\check{H}, \check{V})\|_\infty \to 0$, *where* $\check{V} = \dfrac{\beta_v(x) N_v^* \check{H}}{\mu_v(x)(1-q)N_h^* + \beta_v(x)\check{H}}$ *and* $\check{H} = H^*(L)e^{\frac{-\alpha}{D}(L-x)}$. *In particular,* $H^*(L) \to \kappa^*$, *where* $\kappa^*$ *is the unique positive solution of*

$$e^{\delta\kappa} - (1 + \omega\kappa) = 0, \quad \kappa > 0,$$

*with* $\delta = \dfrac{\beta_v(L)(\frac{\beta_h(L)N_v^*}{N_h^*} + \mu_h(L) + r)}{N_v^*\beta_h(L)(\beta_v(L) + \mu_v(L)(1-q))}$ *and* $\omega = \dfrac{\beta_v(L)}{\mu_v(L)(1-q)N_h^*}$.

(ii) *For each fixed* $\alpha \geq 0$, *we have* $\lim\limits_{D\to+\infty}(H^*(x), V^*(x)) = (\hat{H}, \hat{V})$, *where* $\hat{V} = \dfrac{\beta_v(x)N_v^*\hat{H}}{\mu_v(x)(1-q)N_h^* + \beta_v(x)\hat{H}}$, *and the positive constant* $\hat{H}$ *is the unique positive solution of*

$$\int_0^L \left( \frac{\beta_h(x)\beta_v(x)N_v^*(N_h^* - \hat{H})}{N_h^*(\mu_v(x)(1-q)N_h^* + \beta_v(x)\hat{H})} - (\mu_h(x) + r) \right) \mathrm{d}x = 0.$$

*Proof.* Since

$$V^*(x) = \frac{N_v^*\beta_v(x)H^*(x)}{\mu_v(x)(1-q)N_h^* + \beta_v(x)H^*(x)},$$

it suffices to establish the convergence of $H^*(x)$.

(i) For clarity, the proof is split into three steps as follows.

**Step 1:** Assume $\alpha \geq 2\sqrt{D\Theta_M}$. We claim the estimate

$$e^{\left(\frac{\alpha}{D} + \frac{\tau}{\alpha}\right)(x-L)} \leq \frac{H^*(x)}{H^*(L)} \leq e^{\left(\frac{\alpha}{D} - \frac{2\Theta_M}{\alpha}\right)(x-L)}, \tag{3.4}$$

where $\tau := \frac{\Theta_M M^*}{N_h^*} + \mu_{h,M} + r$ with $\mu_{h,M} = \max\limits_{x\in[0,L]} \mu_h(x)$, and $M^* > 0$ denotes the uniform upper bound of $H^*(x)$. We first verify the left-hand inequality in (3.4).

Set $\underline{H}^*(x) = e^{\left(\frac{\alpha}{D} + \frac{\tau}{\alpha}\right)(x-L)}H^*(L)$. For all $x \in [0, L]$, one has $D\underline{H}_x^* - \alpha\underline{H}^*\big|_{x=0} = \underline{H}^*(0)\frac{D\tau}{\alpha} > 0$. By the definition of $\tau$, straightforward computation yields

$$\begin{aligned}
&D\underline{H}_{xx}^* - \alpha\underline{H}_x^* + \underline{H}^*\left( \frac{\beta_h(x)\beta_v(x)N_v^*(N_h^* - H^*(x))}{N_h^*(\mu_v(x)(1-q)N_h^* + \beta_v(x)H^*(x))} - (\mu_h(x) + r) \right) \\
&= \underline{H}^*(x)\left[ \tau + \frac{D\tau^2}{\alpha^2} + \frac{\beta_h(x)\beta_v(x)N_v^*(N_h^* - H^*(x))}{N_h^*(\mu_v(x)(1-q)N_h^* + \beta_v(x)H^*(x))} - (\mu_h(x) + r) \right] \\
&\geq \underline{H}^*(x)\left[ \tau - \frac{\beta_h(x)\beta_v(x)N_v^*H^*(x)}{N_h^*(\mu_v(x)(1-q)N_h^* + \beta_v(x)H^*(x))} - (\mu_h(x) + r) \right] \\
&\geq \underline{H}^*(x)\left[ \tau - \frac{\Theta_M M^*}{N_h^*} - (\mu_h(x) + r) \right] \geq 0.
\end{aligned}$$

As a consequence, $\underline{H}^*(x)$ satisfies

$$\begin{cases}
D\underline{H}_{xx}^* - \alpha\underline{H}_x^* + \underline{H}^*\left( \frac{\beta_h(x)\beta_v(x)N_v^*(N_h^* - H^*(x))}{N_h^*\left(\mu_v(x)(1-q)N_h^* + \beta_v(x)H^*(x)\right)} - (\mu_h(x) + r) \right) \geq 0, \\
D\underline{H}_x^*(0) - \alpha\underline{H}^*(0) > 0, \quad G(L) = \underline{H}^*(L) - H^*(L) = 0.
\end{cases}$$

Define $G(x) = \underline{H}^*(x) - H^*(x)$ and $T(x) = e^{-\frac{\alpha}{2D}x}G(x)$. Then, $T(x)$ obeys

$$\begin{cases}
DT_{xx} + T\left( \frac{\beta_h(x)\beta_v(x)N_v^*(N_h^* - H^*(x))}{N_h^*\left(\mu_v(x)(1-q)N_h^* + \beta_v(x)H^*(x)\right)} - (\mu_h(x) + r) - \frac{\alpha^2}{4D} \right) \geq 0, \\
DT_x(0) - \frac{\alpha}{2}T(0) > 0, \quad T(L) = 0.
\end{cases}$$

An application of the maximum principle implies $T(x) \le 0$ on $[0, L]$, which is equivalent to $G(x) = \underline{H}^*(x) - H^*(x) \le 0$ on $[0, L]$. This establishes the left-hand bound in (3.4).

We next prove the right-hand inequality of (3.4). Let $\bar{H}^*(x) = H^*(L)e^{\left(\frac{\alpha}{D} - \frac{2\Theta_M}{\alpha}\right)(x-L)}$. Direct evaluation gives

$$D\bar{H}_x^* - \alpha\bar{H}^*\big|_{x=0} = -H^*(L)\frac{2D\Theta_M}{\alpha}e^{-L\left(\frac{\alpha}{D} - \frac{2\Theta_M}{\alpha}\right)} < 0,$$

and

$$\begin{aligned} &D\bar{H}_{xx}^* - \alpha\bar{H}_x^* + \bar{H}^*\left(\frac{\beta_h(x)\beta_v(x)N_v^*(N_h^* - H^*(x))}{N_h^*(\mu_v(x)(1-q)N_h^* + \beta_v(x)H^*(x))} - (\mu_h(x) + r)\right) \\ &\le \bar{H}^*(x)\left[-2\Theta_M + \frac{4D\Theta_M^2}{\alpha^2} + \Theta(x)\right] \le \bar{H}^*(x)\left(\frac{4D\Theta_M^2}{\alpha^2} - \Theta_M\right) \le 0, \end{aligned}$$

where the condition $\alpha \ge 2\sqrt{D\Theta_M}$ is employed. Introduce $P = e^{-\frac{\alpha}{2D}x}(\bar{H}^*(x) - H^*(x))$. Then, $P$ satisfies

$$\begin{cases} DP_{xx} + P\left(\frac{\beta_h(x)\beta_v(x)N_v^*(N_h^* - H^*(x))}{N_h^*\left(\mu_v(x)(1-q)N_h^* + \beta_v(x)H^*(x)\right)} - (\mu_h(x) + r) - \frac{\alpha^2}{4D}\right) < 0, \quad x \in (0, L), \\ DP_x(0) - \frac{\alpha}{2}P(0) < 0, \quad P(L) = 0. \end{cases}$$

Again using $\alpha \ge 2\sqrt{D\Theta_M}$, we have

$$\frac{\beta_h(x)\beta_v(x)N_v^*(N_h^* - H^*(x))}{N_h^*(\mu_v(x)(1-q)N_h^* + \beta_v(x)H^*(x))} - (\mu_h(x) + r) - \frac{\alpha^2}{4D} < \Theta(x) - \frac{\alpha^2}{4D} \le \Theta_M - \frac{\alpha^2}{4D} \le 0.$$

By the maximum principle, $P(x) \ge 0$, that is, $\bar{H}^*(x) - H^*(x) \ge 0$. The right-hand estimate in (3.4) thus follows.

**Step 2:** Convergence of $H^*(x)$. From inequality (3.4), one derives

$$H^*(L)e^{-\frac{\alpha}{D}(L-x)}(e^{\frac{\tau}{\alpha}(x-L)} - 1) \le H^*(x) - H^*(L)e^{-\frac{\alpha}{D}(L-x)} \le H^*(L)e^{-\frac{\alpha}{D}(L-x)}(e^{\frac{2\Theta_M}{\alpha}(L-x)} - 1).$$

Consequently, in the advection-dominated regime, we obtain $\|H^*(x) - H^*(L)e^{-\frac{\alpha}{D}(L-x)}\|_{L^\infty(0,L)} \to 0$.

**Step 3:** Convergence of $H^*(L)$. Recall that the rescaled function $\tilde{\mathbf{H}}(y)$ satisfies Eq (3.1). For $\alpha \ge 2\sqrt{D\Theta_M}$, combining estimate (3.4) with the normalization condition $\tilde{\mathbf{H}}(0) = 1$, we derive the pointwise bounds

$$e^{-y\left(1+\frac{D\tau}{\alpha^2}\right)} \le \tilde{\mathbf{H}}(y) \le e^{-y\left(1-\frac{2D\Theta_M}{\alpha^2}\right)}, \quad y \in \left(0, \frac{\alpha L}{D}\right).$$

Accordingly, $\tilde{\mathbf{H}}(y) \to e^{-y}$ pointwise in $y$ in the above advection-dominated regime. By Lemma 3.2, $H^*(L) = \mathbf{H}(0)$ is uniformly bounded along this regime. By passing to a subsequence, we may suppose $\mathbf{H}(0) \to \kappa$ along this regime. Let $s := e^{-y}$. With the aid of Lemma 3.2 and identity (3.3), we obtain

$$\begin{aligned} 0 &= \int_0^\infty e^{-y}\left(\frac{N_v^*\beta_h(L)\beta_v(L)(N_h^* - e^{-y}\mathbf{H}(0))}{N_h^*(\mu_v(L)(1-q)N_h^* + \beta_v(L)e^{-y}\mathbf{H}(0))} - (\mu_h(L) + r)\right)\mathrm{d}y \\ &= \int_0^1 \left(\frac{N_v^*\beta_h(L)\beta_v(L)(N_h^* - s\kappa)}{N_h^*(\mu_v(L)(1-q)N_h^* + \beta_v(L)s\kappa)} - (\mu_h(L) + r)\right)\mathrm{d}s \\ &= -\left(\frac{N_v^*\beta_h(L)}{N_h^*} + \mu_h(L) + r\right) + \frac{N_v^*\beta_h(L)(\beta_v(L) + \mu_v(L)(1-q))}{\beta_v(L)\kappa}\ln\left(1 + \frac{\beta_v(L)\kappa}{N_h^*\mu_v(L)(1-q)}\right). \end{aligned}$$

Define the constants

$$\delta = \frac{\beta_v(L)\left(\frac{\beta_h(L)N_v^*}{N_h^*} + \mu_h(L) + r\right)}{N_v^*\beta_h(L)(\beta_v(L) + \mu_v(L)(1-q))}, \qquad \omega = \frac{\beta_v(L)}{\mu_v(L)(1-q)N_h^*}.$$

It remains to verify that the scalar equation $f(\kappa) = e^{\delta\kappa} - (1 + \omega\kappa) = 0$ admits exactly one positive root in $(0, +\infty)$. We first establish the inequality $\delta < \omega$ via direct computation as follows:

$$\begin{aligned}\delta - \omega &= \frac{\beta_v(L)\mu_v(L)(1-q)N_h^*\left(\frac{\beta_h(L)N_v^*}{N_h^*} + \mu_h(L) + r\right) - \beta_v(L)N_v^*\beta_h(L)(\beta_v(L) + \mu_v(L)(1-q))}{N_v^*\beta_h(L)(\beta_v(L) + \mu_v(L)(1-q))\mu_v(L)(1-q)N_h^*} \\ &= \frac{\beta_v(L)\left[\mu_v(L)(1-q)N_h^*(\mu_h(L) + r) - N_v^*\beta_h(L)\beta_v(L)\right]}{N_v^*\beta_h(L)(\beta_v(L) + \mu_v(L)(1-q))\mu_v(L)(1-q)N_h^*} < 0,\end{aligned}$$

where the last inequality follows from $r < \theta^* \leq \theta(L)$. Consequently, $\ln\frac{\omega}{\delta} > 0$. Differentiating yields $f'(\kappa) = \delta e^{\delta\kappa} - \omega$, so

$$\begin{aligned} f'(\kappa) < 0, &\quad 0 < \kappa < \frac{1}{\delta}\ln\frac{\omega}{\delta}, \\ f'(\kappa) = 0, &\quad \kappa = \frac{1}{\delta}\ln\frac{\omega}{\delta}, \\ f'(\kappa) > 0, &\quad \kappa > \frac{1}{\delta}\ln\frac{\omega}{\delta}. \end{aligned}$$

Combining $f(0) = 0$ and $\lim\limits_{\kappa\to+\infty} f(\kappa) = +\infty$, we conclude that $f(\kappa) = 0$ possesses a unique positive solution.

(ii) Since $H^*(x)$ satisfies (2.3) and remains uniformly bounded as $D \to +\infty$, we divide both sides of Eq (2.3) by $D$ and integrate from 0 to $x$. This yields

$$H_x^* - \frac{\alpha}{D}H^* + \frac{1}{D}\int_0^x H^*(s)\left(\frac{\beta_h(s)\beta_v(s)N_v^*(N_h^* - H^*(s))}{N_h^*(\mu_v(s)(1-q)N_h^* + \beta_v(s)H^*(s))} - (\mu_h(s) + r)\right)\mathrm{d}s = 0,$$

which implies $H_x^* \to 0$ for all $x \in [0, L]$ as $D \to +\infty$. Substituting back into (2.3), we further deduce $H_{xx}^* \to 0$ on $[0, L]$ in the same limiting regime. Thus, as $D \to +\infty$, by passing to a subsequence, we may assume that $H^*(x)$ uniformly converges to a positive constant $\hat{H}$ on $[0, L]$. Integrating the equation for $H^*(x)$ over $(0, L)$, we obtain

$$\int_0^L H^*(x)\left(\frac{\beta_h(x)\beta_v(x)N_v^*(N_h^* - H^*(x))}{N_h^*(\mu_v(x)(1-q)N_h^* + \beta_v(x)H^*(x))} - (\mu_h(x) + r)\right)\mathrm{d}x = 0,$$

so the limit $\hat{H}$ satisfies

$$g(\hat{H}) := \int_0^L \left(\frac{\beta_h(x)\beta_v(x)N_v^*(N_h^* - \hat{H})}{N_h^*(\mu_v(x)(1-q)N_h^* + \beta_v(x)\hat{H})} - (\mu_h(x) + r)\right)\mathrm{d}x = 0.$$

When $0 < r < \theta^*$, direct evaluation yields $g(0) = \int_0^L(\theta(x) - r)\mathrm{d}x > 0$ and $g(2N_h^*) < 0$. It can be readily verified from its definition that $g(\hat{H})$ is strictly decreasing in $\hat{H}$. Hence, there exists a unique positive root $\hat{H} > 0$ solving $g(\hat{H}) = 0$, which finishes the proof. □

## 4. Numerical simulations

In this section, we use numerical simulations to illustrate the analytical results in Theorem 3.3 and to further examine the effects of diffusion and advection on the endemic steady state of system (1.2).

We set

$$L = 1, \qquad q = 0.03, \qquad N_h^* = 200, \qquad N_v^* = 240,$$

and choose

$$\beta_h(x) = 0.5 + 0.1\sin(\pi x), \qquad \beta_v(x) = 0.4 + 0.05x, \qquad \mu_h(x) = 0.1 + 0.02x, \qquad \mu_v = 0.15.$$

For these parameter values, one obtains $\theta^* \approx 0.94$. We therefore take $r = 0.2$, so that the condition $0 < r < \theta^*$ is satisfied.

Figure 1 shows the effects of the diffusion rate $D$ on the maximal infected densities $\max H(x)$ and $\max V(x)$ for three fixed advection rates $\alpha = 0.5, 2, 5$. For each fixed $\alpha$, the maximal infected densities decrease as $D$ increases over the sampled range. This is consistent with the large-diffusion limit in Theorem 3.3(ii): Strong diffusion tends to homogenize the infected bird density, so that $H^*(x)$ approaches a positive spatially homogeneous limit $\hat{H}$. The corresponding infected mosquito density is then determined by the local transmission relation

$$\hat{V}(x) = \frac{\beta_v(x)N_v^*\hat{H}}{\mu_v(x)(1-q)N_h^* + \beta_v(x)\hat{H}},$$

which may still depend on $x$ through the spatially heterogeneous coefficients. In contrast, when $D$ is small, diffusion is weak and the effect of advection is more pronounced, leading to stronger downstream accumulation of infection near $x = L$. Larger values of $\alpha$ enhance this directional effect and result in higher maximal infected densities under the same diffusion level.

Figure 2 illustrates the effects of the advection rate $\alpha$ on $\max H(x)$ and $\max V(x)$ for three fixed diffusion rates (i.e., $D = 0.05, 1$ *and* $5$). As $\alpha$ increases, directional advection shifts the infected bird density toward the right boundary and promotes downstream accumulation. Consequently, the maximal infected densities increase and then approach limiting values. For small $D$, advection dominates diffusion more strongly, and the curves rise rapidly before reaching a plateau. This behavior agrees with the boundary-layer description in Theorem 3.3(i): as $\alpha \to +\infty$, the infected bird density is approximated by

$$\check{H}(x) = H^*(L)\exp\left(-\frac{\alpha}{D}(L-x)\right),$$

where $H^*(L)$ converges to the unique positive constant $\kappa^*$. For larger $D$, diffusion counteracts the downstream accumulation induced by advection, so the increase in the maximal infected densities is milder.

We next investigate the relationship between spatial distribution and diffusion under a fixed advection rate $\alpha = 1$. The parameters are set as follows: $L = 1$, $N_h^* = 12$, $N_v^* = 12$, $r = 0.35$, $q = 0.02$, $\beta_h(x) = 0.3 + 1.0x$, $\beta_v(x) = 0.2 + 1.2x$, $\mu_h(x) = 0.15 + 0.12x$, and $\mu_v(x) = 0.4 + 0.35x$. Under these settings, $\theta^* = 1.1$ satisfies $0 < r = 0.35 < \theta^*$. As shown in Figure 3, for $D = 0.1$: Weak diffusion lets advection concentrate $H^*(x)$ near $x = 1$. Substituting heterogeneous $H$ into $V(x) = \frac{\beta_v N_v^* H}{\mu_v(1-q)N_h^* + \beta_v H}$ yields spatially varying $V$; for $D = 5$: Moderate diffusion weakens boundary accumulation and smooths both

$H^*(x)$ and $V^*(x)$; for $D = 500$: Large diffusion homogenizes $H^*(x) \equiv \hat{H}$. However, space-dependent $\beta_v(x), \mu_v(x)$ retain mild spatial variation in $V^*(x)$, showing uniform host density does not imply uniform mosquito density.

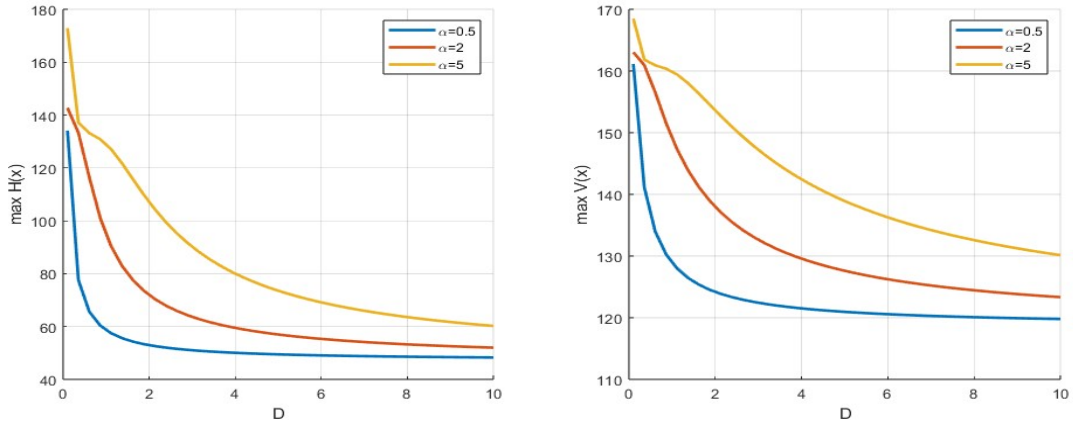


**Figure 1.** Numerical results in the large-diffusion regime, depicting the dependence of $\max H(x)$ and $\max V(x)$ on diffusion rate $D$ for fixed advection strengths $\alpha = 0.5, 2, 5$. The descending tendency of maximal infected densities with growing $D$ verifies the homogenization asymptotic behavior established in Theorem 3.3 (ii). Other parameter values are $L = 1$, $q = 0.03$, $N_h^* = 200$, $N_v^* = 240$, $\beta_h(x) = 0.5 + 0.1\sin(\pi x)$, $\beta_v(x) = 0.4 + 0.05x$, $\mu_h(x) = 0.1 + 0.02x$, $\mu_v = 0.15$, and $r = 0.2$.

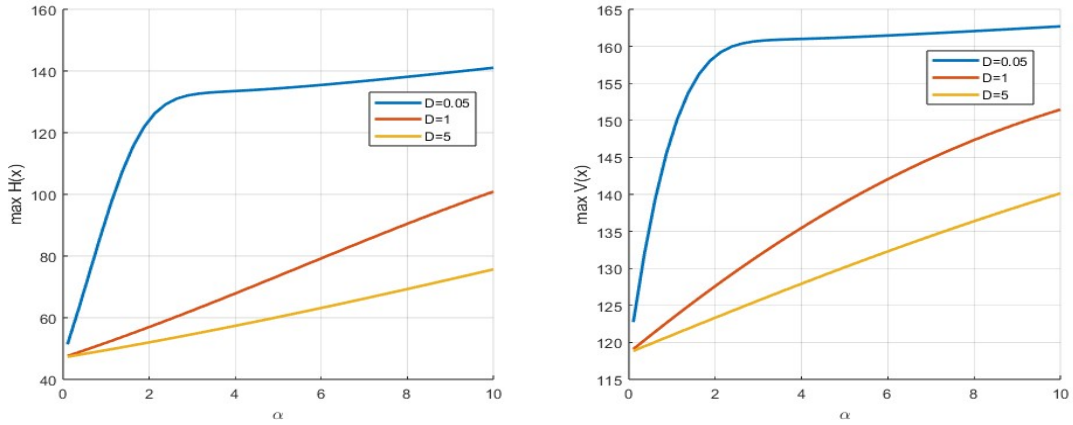


**Figure 2.** Numerical results in the advection-dominated regime, illustrating how advection strength $\alpha$ affects $\max H(x)$ and $\max V(x)$ under fixed diffusion levels $D = 0.05, 1, 5$. The rising saturation curves confirm the boundary-layer asymptotic properties derived in Theorem 3.3 (i). All remaining parameter values are identical to those adopted in Figure 1.

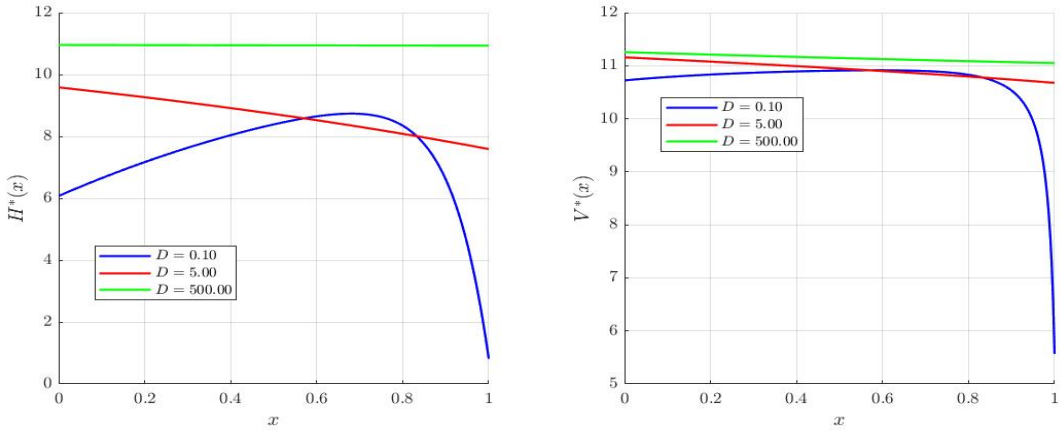


**Figure 3.** Spatial steady-state profiles of infected bird density $H^*(x)$ (left) and infected mosquito density $V^*(x)$ (right) with fixed $\alpha = 1$ and three distinct diffusion coefficients $D = 0.1, 5, 500$. Other parameters values: $L = 1$, $N_h^* = 12$, $N_v^* = 12$, $r = 0.35$, $q = 0.02$, $\beta_h(x) = 0.3 + 1.0x$, $\beta_v(x) = 0.2 + 1.2x$, $\mu_h(x) = 0.15 + 0.12x$ *and* $\mu_v(x) = 0.4 + 0.35x$,

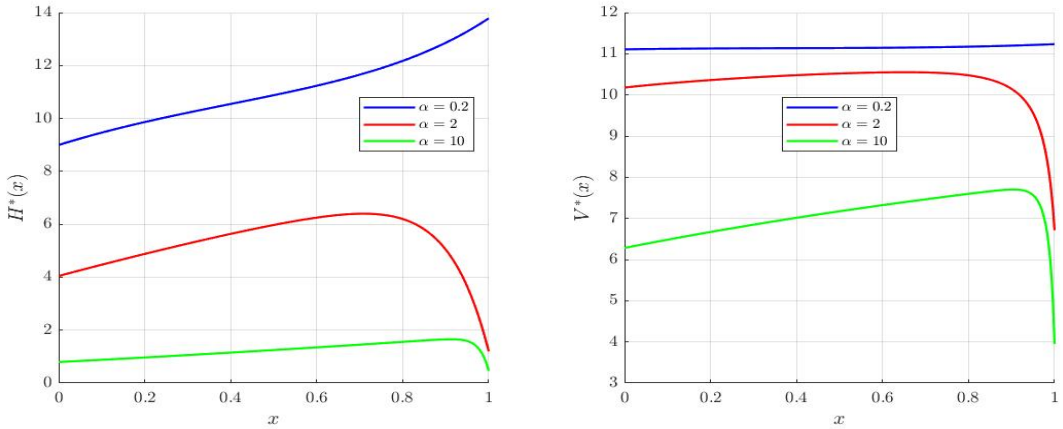


**Figure 4.** Spatial steady-state profiles of infected bird density $H^*(x)$ (left) and infected mosquito density $V^*(x)$ (right) with fixed $D = 0.2$ and three distinct diffusion coefficients $\alpha = 0.2, 2, 10$. Other parameters values: $L = 1$, $N_h^* = 12$, $N_v^* = 12$, $r = 0.35$, $q = 0.02$, $\beta_h(x) = 0.3 + 1.0x$, $\beta_v(x) = 0.2 + 1.2x$, $\mu_h(x) = 0.15 + 0.12x$ *and* $\mu_v(x) = 0.4 + 0.35x$,

On the other hand, We study the relationship between spatial distribution and advection under a fixed diffusion rate $D = 0.2$. The parameters are set as follows: $L = 1$, $N_h^* = 12$, $N_v^* = 12$, $r = 0.35$, $q = 0.02$, $\beta_h(x) = 0.3 + 1.0x$, $\beta_v(x) = 0.2 + 1.2x$, $\mu_h(x) = 0.15 + 0.12x$, and $\mu_v(x) = 0.4 + 0.35x$. Under these settings, $\theta^* = 1.1$ satisfies $0 < r = 0.35 < \theta^*$. By Figure 4, we see that

- $\alpha = 0.2$: Weak advection barely drives rightward aggregation. $H^*(x)$ rises gently without boundary peak, and $V^*(x)$ is nearly uniform.
- $\alpha = 2$: Moderate advection accumulates hosts near $x = 1$, forming a visible hump of $H^*(x)$. $V(x) = \frac{\beta_v N_v^* H}{\mu_v(1-q)N_h^* + \beta_v H}$ inherits this boundary enrichment.
- $\alpha = 10$: Strong advection concentrates most infected hosts within a thin boundary layer at $x = 1$.

The bulk value of $H^*(x)$ decreases significantly, while $V^*(x)$ also shrinks overall but still peaks at the right endpoint, consistent with the boundary-layer asymptotic behavior as $\alpha \to +\infty$.

## 5. Conclusions

This paper investigated the effects of diffusion and advection on endemic steady states in a partially degenerate West Nile virus model. The infected bird density satisfies a diffusion-advection equation, whereas the infected mosquito density is determined at steady state by a local host-vector transmission balance. This elliptic-algebraic structure requires a steady-state analysis different from that for fully diffusive epidemic systems.

Under the condition $\theta^* > 0$ and $0 < r < \theta^*$, we established the existence and uniqueness of a positive endemic steady state. We then derived two limiting descriptions of the endemic spatial profile. In the advection-dominated regime, including large advection and vanishing diffusion with fixed positive advection, the infected bird density develops a downstream boundary layer of the form

$$H^*(x) \sim H^*(L)e^{-\frac{\alpha}{D}(L-x)}.$$

Moreover, the limiting boundary value $H^*(L)$ is determined by a scalar equation. In the large-diffusion regime, the infected bird density converges to a positive spatially homogeneous state, whereas the corresponding infected mosquito density is determined by the local transmission relation and may remain spatially heterogeneous.

These two limiting regimes suggest different qualitative implications for spatial disease surveillance and control. When directional bird movement is strong, the boundary-layer profile predicts that infected birds, and consequently locally generated mosquito infections, may become concentrated near the boundary toward which the advective transport is directed, namely $x = L$ in the present setting. Subject to site-specific parameter estimation and field validation, this observation suggests that surveillance of infected birds and mosquitoes, reduction of mosquito breeding habitats, and other vector-control measures could place greater emphasis on such downstream accumulation zones. By contrast, when bird diffusion is sufficiently large, the infected bird density becomes nearly homogeneous throughout the habitat. This regime may be viewed as an idealized analogue of a highly connected or effectively well-mixed environment, in which endemic infection is spatially widespread rather than confined to a pronounced hotspot. In such a setting, spatially distributed surveillance may be more appropriate than control focused on a single location. It is important, however, that the mosquito infection profile need not become homogeneous, since it still reflects the spatial variation of local transmission and mortality rates. Thus, strong avian mixing may redistribute endemic infection without necessarily eliminating local heterogeneity in vector-associated risk.

These interpretations are qualitative and should not be regarded as direct public-health recommendations without site-specific calibration and empirical validation. In particular, the present model does not explicitly incorporate mosquito movement, control interventions, seasonal variation, or detailed landscape structure. Possible extensions therefore include mosquito diffusion, seasonal forcing, nonlocal bird movement, intervention terms, and spatial coefficients informed by ecological and epidemiological data.

## Author contributions

Jie Xing: Writing-original draf; Lin Wang: Writing-original draf, Writing-review and editing. All authors have read and approved the final version of the manuscript for publication.

## Use of Generative-AI tools declaration

The authors declare they have not used Artificial Intelligence (AI) tools in the creation of this article.

## Acknowledgments

We are grateful to the handling editor and anonymous referee for careful reading and valuable comments which led to improvements of our original manuscript. JX is partially supported by the Natural Science Foundation of Guangxi (Grant PF260249), the Science and Technology Project of Guangxi (Guike AD25069086), and the research initiation project of Guilin University of Electronic Technology (Grant UF25085Y). LW is partially supported by Research initiation project of Jimei University (ZQ2025018).

## Conflict of interest

The author declares that she has no conflict of interest.

## References

1. C. Bowman, A. B. Gumel, P. van den Driessche, J. Wu, H. Zhu, A mathematical model for assessing control strategies against West Nile virus, *Bull. Math. Biol.*, **67** (2005), 1107–1133. https://doi.org/10.1016/j.bulm.2005.01.002
2. D. J. Dohm, M. R. Sardelis, M. J. Turell, Experimental vertical transmission of West Nile virus by Culex pipiens (Diptera: Culicidae), *J. Med. Entomol.*, **39** (2002), 640–644. https://doi.org/10.1603/0022-2585-39.4.640
3. R. S. Cantrell, C. Cosner, *Spatial ecology via reaction-diffusion equations*, United States: John Wiley & Sons, 2004. https://doi.org/10.1002/0470871296
4. K. Deimling, *Nonlinear functional analysis*, Berlin: Springer-Verlag, 1985. https://doi.org/10.1007/978-3-662-00547-7
5. J. Ge, Z. Lin, H. Zhu, Modeling the spread of West Nile virus in a spatially heterogeneous and advective environment, *J. Appl. Anal. Comput.*, **11** (2021), 1868–1897. https://doi.org/10.11948/20200258
6. L. C. Harrington, T. W. Scott, K. Lerdthusnee, R. C. Coleman, A. Costero, G. G. Clark, et al., Dispersal of the dengue vector Aedes aegypti within and between rural communities, *Am. J. Trop. Med. Hyg.*, **72** (2005), 209–220. https://doi.org/10.4269/ajtmh.2005.72.209
7. J. Jiang, Z. Qiu, The complete classification for dynamics in a nine-dimensional West Nile virus model, *SIAM J. Appl. Math.*, **69** (2009), 1205–1227. https://doi.org/10.1137/070709438

8. J. Jiang, Z. Qiu, J. Wu, H. Zhu, Threshold conditions for West Nile virus outbreaks, *Bull. Math. Biol.*, **71** (2009), 627–647. https://doi.org/10.1007/s11538-008-9374-6
9. M. A. Lewis, J. Renclawowicz, P. van den Driessche, Traveling waves and spread rates for a West Nile virus model, *Bull. Math. Biol.*, **68** (2006), 3–23. https://doi.org/10.1007/s11538-005-9018-z
10. Z. Lin, H. Zhu, Spatial spreading model and dynamics of West Nile virus in birds and mosquitoes with free boundary, *J. Math. Biol.*, **75** (2017), 1381–1409. https://doi.org/10.1007/s00285-017-1124-7
11. C. C. Lord, J. F. Day, Simulation studies of St. Louis encephalitis and West Nile viruses: the impact of bird mortality, *Vect. Borne Zoon. Dis.*, **1** (2001), 317–329. https://doi.org/10.1089/15303660160025930
12. P. Magal, X. Q. Zhao, Global attractors and steady states for uniformly persistent dynamical systems, *SIAM J. Math. Anal.*, **37** (2005), 251–275. https://doi.org/10.1137/S0036141003439173
13. N. A. Maidana, H. M. Yang, Spatial spreading of West Nile virus described by traveling waves, *J. Theor. Biol.*, **258** (2009), 403–417. https://doi.org/10.1016/j.jtbi.2008.12.032
14. K. C. Smithburn, T. P. Hughes, A. W. Burke, J. H. Paul, A neurotropic virus isolated from the blood of a native of Uganda, *Am. J. Trop. Med.*, **20** (1940), 471–492. https://doi.org/10.4269/ajtmh.1940.s1-20.471
15. D. M. Thomas, B. Urena, A model describing the evolution of West Nile-like encephalitis in New York City, *Math. Comput. Model.*, **34** (2001), 771–781. https://doi.org/10.1016/S0895-7177(01)00098-X
16. J. Wang, H. Nie, Invasion dynamics of a predator-prey system in closed advective environments, *J. Differ. Equations*, **318** (2022), 298–322. https://doi.org/10.1016/j.jde.2022.02.043
17. M. J. Wonham, T. de-Camino-Beck, M. A. Lewis, An epidemiological model for West Nile virus: invasion analysis and control applications, *Proc. R. Soc. Lond. B*, **271** (2004), 501–507. https://doi.org/10.1098/rspb.2003.2608
18. J. Xing, H. Nie, J. Wu, On a partially degenerate West Nile virus model in closed advective environments, *Z. Angew. Math. Phys.*, **76** (2025), 13. https://doi.org/10.1007/s00033-024-02402-9


AIMS Press